

Predicting property damage from tornadoes with deep learning

Jeremy Diaz^{a*}, Maxwell Joseph^a

^aEarth Lab, University of Colorado Boulder. 4001 Discovery Drive Suite S348 – UCB 611. Boulder, CO 80303.

*Corresponding author. *E-mail address:* jeremy.diaz@colorado.edu

Abstract

Tornadoes are the most violent of all atmospheric storms. In a typical year, the United States experiences hundreds of tornadoes with associated damages on the order of one billion dollars. Community preparation and resilience would benefit from accurate predictions of these economic losses, particularly as populations in tornado-prone areas continue to increase in density and extent. Here, we use artificial neural networks to predict tornado-induced property damage using publicly available data. We find that the large number of tornadoes which cause zero property damage (30.6% of the data) poses a challenge for predictive models. We developed a model that predicts whether a tornado will cause property damage to a high degree of accuracy (out of sample accuracy = 0.829 and AUROC = 0.873). Conditional on a tornado causing damage, another model predicts the amount of damage. When combined, these two models yield an expected value for the amount of property damage caused by a tornado event. From the best-performing models (out of sample mean squared error = 0.089 and $R^2 = 0.473$), we provide an interactive, gridded map of monthly expected values for the year 2018. One major weakness is that the model predictive power is optimized with log-transformed, mean-normalized property damages, however this leads to large natural-scale residuals for the most destructive tornadoes. The predictive capacity of this model along with an interactive interface may provide an opportunity for science-informed tornado disaster planning.

Keywords

Tornadoes; Machine learning; Property damage; Artificial neural networks; Predictive modelling; United States.

1. Introduction

The United States experiences more tornadoes every year than any other country in the world, with the annual average of cumulative tornado-induced property damage at nearly one billion US dollars [1]. However, the distribution of property damages is heavy-tailed: the annual average has been exceeded by costs from single severe tornadoes, such as the 2011 Joplin tornado, which caused \$2.8 billion dollars in damages [2]. The damages resulting from tornadoes is a function of the physical properties of storms and societal factors such as population density, property values, and quality of housing [3, 4, 5]. Independent of physical changes in the number, distribution, or intensity of tornadoes, increasing property values, population density, and manufactured home density may contribute to observed increases in

tornado damages in recent decades [3, 4, 5, 6, 7, 8]. These societal factors may be useful for predicting future tornado damages under different scenarios, with applications to development planning [9], natural disaster asset prepositioning [10], refinement of public warning systems [11], the property-casualty insurance industry [1], and disaster response coordination [12].

Here, we model tornado-induced property damages from the NOAA Storm Events Database as a function of 35 known and hypothesized drivers of damages, compiled from publicly available data. While previous research has identified variables that may be important [3, 4, 5, 6, 7, 8], the assumption of linearity in the effects is limiting [13]. The functional relationships among these proposed drivers and tornado damages are uncertain and possibly nonlinear, requiring a flexible means of predicting future observations as an unknown function of possibly interacting inputs. We use artificial neural networks to predict tornado-induced property damage over the past 20 years as a function of explanatory variables identified in the tornado risk literature.

The universal function approximation capacity of artificial neural networks [14, 15] may provide a means to learn the possibly complex functional relationships between proposed drivers and property damage. Previously, neural networks have been employed to predict the occurrence of tornadoes from radar data [16, 17], and the occurrence of damaging winds [18]. Conditional on the occurrence of a natural disaster, neural networks have proved useful for assessing damages, for instance after the December 2004 tsunami in Aceh, Sumatra [19]. The application of machine learning to the prediction of potential tornado damages appears promising, though nascent in the current literature.

The NOAA Storm Events Database provides an opportunity to train a model with historical tornado-induced property damages with the goal of generating future predictions that are useful for disaster relief and development scenario-analysis. Along with predictions of future tornado-induced property damages, we present prototype dashboards that communicate these predictions in a way that could be used by planners without expertise in machine learning or spatial analysis [20].

2. Methods

2.1. Data acquisition and processing

To develop the predictive models, we acquired data from past tornado events from NOAA's Storm Events Database (hereafter "Storm Events") [21], which includes information about where and when a tornado occurred, tornado path length and width, and how much property damage it caused. Due to the increased frequency of tornado reporting and changes in the reporting of tornado path width, we did not consider any tornadoes occurring before 1997 [22]; Additionally, the most recent tornadoes considered occurred on August 31, 2017.

For each tornado event, we extracted land cover classes from the USGS/DOI National Land Cover Database (hereafter “NLCD”) [23, 24, 25]. The NLCD is not updated annually, so we used the 2001 land cover classes for all tornado events occurring before 2001, the 2006 classes for events occurring between 2006 and 2011, and the 2011 classes for events occurring after 2011. The buffer radius for land cover class extraction was 5093.071 meters, the average length of tornadoes recorded in Storm Events. From the resulting list of land cover classifications, we calculated the proportion of each classification within the buffer radius for each event. We then removed an erroneous NLCD classification “0” which is not a documented classification in the NLCD. Last, we removed the outlying “Perennial Ice/Snow” classification, because it only appeared in 0.01% of the tornado events.

To capture relevant socioeconomic factors that might explain tornado damages, we acquired median household income, total population count, and total mobile home data by county using the American Community Survey’s (ACS) [26] 5 year estimates (via the tidycensus R package, <https://cran.r-project.org/web/packages/tidycensus/index.html>). The United States Census Bureau’s (USCB) Land Area data set [27] was then used to calculate densities of the ACS-provided mobile home and population counts. Data before 2009 and after 2015 are not yet available from the ACS, so we assumed values before 2009 to be equal to the 2009 values, while values after 2015 were equal to the 2015 values. All ACS/USCB variables were integrated into the data set by matching county, state, and year with the tornado events.

There were some inconsistencies among the data sources’ county names that made it impossible to match a tornado event to an explanatory variable. When these occurred, they resulted in missing values during the data set matchings. All missing values were omitted before the analysis. These inconsistencies occurred for less than 1% of the tornadoes in Storm Events, and as they were due to misspellings of county-level names, we can assume that the missingness mechanism is independent of the response of interest, so discarding the events with missing covariates is unlikely to lead to systematic bias in the filtered data.

2.2. Derived explanatory variables

After all data sources were integrated into the data set, we produced several derived explanatory variables that we expected to be predictive of tornado damages. “Tornado Area” is the product of “Tornado Length” and “Tornado Width”. “State Rank” was a way to numerically and more-informatively incorporate the state of the tornado event; each state name was replaced with its state’s ranking in Storm Events-determined cumulative tornado-induced property damage since January 1st, 1997. Multi-vortex tornadoes tend to cause more severe damage [28], so we performed a text-search on the Storm Event’s “event narratives” to determine whether or not a tornado was a multi-vortex tornado; this is represented in the binary “Multi-Vortex Indicator” variable. “Beginning Time” and “Day of the Year” are both represented as basis expansions using cubic splines with 8 and 12 evenly spaced knots over minutes since midnight and day of the year, respectively.

“Total Developed Intensity” is the sum of each “Developed” land cover proportion multiplied by the median value of that classification’s impervious surface cover (as given in https://www.mrlc.gov/nlcd06_leg.php). “Total Wooded Proportion” is the sum of the “Woody” and “Forest” classification portions, and “Total Wooded-Developed Interaction” is the product of “Total Developed Intensity” and “Total Wooded Proportion”. Lastly, “Total Income Estimate for Tornado Area” is the product of “Tornado Area” and “Estimate of Median Income (county)”. All variables, along with their data source(s), references, and processing methods, are named in **Table 1**.

Data Source	Variable Name	Reference	Processing
Storm Events	Property Damage*		$\frac{\log_e(X+1) - \bar{X}}{S_x}$
	Tornado Duration		$\frac{\log_e(X+1) - \bar{X}}{S_x}$
	Beginning Latitude	[7, 29-32]	$\frac{X - \bar{X}}{S_x}$
	Beginning Longitude	[7, 29-32]	$\frac{X - \bar{X}}{S_x}$
	State Rank**	[7, 29-32]	$\frac{\log_e(1000 * X + 1) - \bar{X}}{S_x}$
	Tornado Length		$\frac{\log_e(X+1) - \bar{X}}{S_x}$
	Tornado Width		$\frac{\log_e(X+1) - \bar{X}}{S_x}$
	Tornado Area*		$\frac{\log_e(1000 * X + 1) - \bar{X}}{S_x}$
	Multi-Vortex Indicator**	[28]	
	Beginning Time of Tornado Event (bs)	[6, 29]	$\frac{\log_e(1000 * X + 1) - \bar{X}}{S_x}$
	Year of Tornado Event	[6, 31]	$\frac{X - \bar{X}}{S_x}$
	Day of the Year of Tornado Event (bs)	[6, 29-32]	$\frac{\log_e(1000 * X + 1) - \bar{X}}{S_x}$
	NLCD	Open Water Proportion	
Developed Open Space Proportion		[6-8]	$\frac{\log_e(1000 * X + 1) - \bar{X}}{S_x}$
Developed Low Intensity Proportion		[6-8]	$\frac{\log_e(1000 * X + 1) - \bar{X}}{S_x}$
Developed Medium Intensity Proportion		[6-8]	$\frac{\log_e(1000 * X + 1) - \bar{X}}{S_x}$
Developed High Intensity Proportion		[6-8]	$\frac{\log_e(1000 * X + 1) - \bar{X}}{S_x}$
Barren Land Proportion			$\frac{\log_e(1000 * X + 1) - \bar{X}}{S_x}$
Deciduous Forest Proportion		[6]	$\frac{\log_e(1000 * X + 1) - \bar{X}}{S_x}$

	Evergreen Forest Proportion	[6]	$\frac{\log_e(1000 * X + 1) - \bar{X}}{Sx}$
	Mixed Forest Proportion	[6]	$\frac{\log_e(1000 * X + 1) - \bar{X}}{Sx}$
	Shrub/Scrub Proportion		$\frac{\log_e(1000 * X + 1) - \bar{X}}{Sx}$
	Grassland/Herbaceous Proportion		$\frac{\log_e(1000 * X + 1) - \bar{X}}{Sx}$
	Pasture/Hay Proportion		$\frac{\log_e(1000 * X + 1) - \bar{X}}{Sx}$
	Cultivated Crops Proportion		$\frac{\log_e(1000 * X + 1) - \bar{X}}{Sx}$
	Woody Wetland Proportion	[6]	$\frac{\log_e(1000 * X + 1) - \bar{X}}{Sx}$
	Emergent Herbaceous Wetland Proportion		$\frac{\log_e(1000 * X + 1) - \bar{X}}{Sx}$
	Total Developed Intensity**	[6-7]	$\frac{\log_e(1000 * X + 1) - \bar{X}}{Sx}$
	Total Wooded Proportion**	[6]	$\frac{\log_e(1000 * X + 1) - \bar{X}}{Sx}$
	Total Wooded-Developed Interaction**		$\frac{\log_e(1000 * X + 1) - \bar{X}}{Sx}$
ACS	Estimate of Median Income (county)	[3-4]	$\frac{\log_e(X + 1) - \bar{X}}{Sx}$
ACS, USCB	Mobile Home Density	[5, 29]	$\frac{\log_e(1000 * X + 1) - \bar{X}}{Sx}$
ACS, USCB	Population Density	[3, 4, 29]	$\frac{\log_e(X + 1) - \bar{X}}{Sx}$
Storm Events, ACS	<i>Total Income Estimate for Tornado Area**</i>	[3-4]	$\frac{\log_e(X + 1) - \bar{X}}{Sx}$

Table 1. All Variables used in the predictive modelling, their sources, their processing method, and, if applicable, their literature justification. "Property Damage" contains an asterisk (*) to indicate that it is the outcome variable, while double asterisks (**) indicate derived variables. Bolded variable names indicate variables which can be known given only a location; i.e., without tornado/storm information. "Total Income Estimate for Tornado Area" is italicized to indicate that it is a mixture of location and tornado/storm information and, therefore, only used in combined models. A variable name followed by (bs) indicates that it was represented by a cubic B-spline expansion. The processing column contains the formula describing how the variable was transformed before being used in the models; \bar{X} represents the sample mean, while Sx represents the sample standard deviation.

2.3. Data Processing and Handling

To avoid ill-conditioning and stabilize parameter learning, all variables were processed to have mean zero and unit standard deviation. To promote trend learning, variables with high variance were preprocessed with log transformations to further centralize distributions. All processing formulas are provided in **Table 1**.

After processing, the data were randomly partitioned into three sets: a training set (consisting of a randomly selected 60% of events), cross-validation set (20%), and test set (20%). The training set was used to optimize the model coefficients/parameters, while the cross-validation set was used to determine the best model among those of differing hyperparameters (such as neural network architecture and regularization strength), and the test set was used as a final determination of the best model's predictive performance. At each stage, predictive performance was measured as mean squared error (MSE) between predicted and true property damage values.

2.4. The Models

All models were made in the PyTorch deep learning framework (<http://pytorch.org/>). These models were produced using the mini-batch gradient descent optimization algorithm, along with the AdaGrad parameter-updating method [33], and rectified linear unit (ReLU) activation functions (except for on the output layers, which had an identity function).

We initially considered three variable-set models: (1) “beforehand” models excluded all variables regarding the tornado event, these variables are shown in bold font in **Table 1**; (2) “storm characteristic” models excluded all variables regarding the location of the tornado (such as county income and population density), these variables are shown in normal font in **Table 1**; and (3) “combined models” used all the variables contained in both (1) and (2) with the addition of a “Total Income Estimate for Tornado Area” variable (which entails both location and tornado information).

For each model type, we developed several artificial neural networks. Artificial networks were made with a two-thirds descending number of neurons per hidden layer until a layer contained only 4 neurons (if a descent led to less than 4 neurons, it was rounded up to 4), and this layer was then connected to a one-neuron output layer. Non-integer values produced by the descent were rounded to the nearest integer, and that new integer then was used in determining the subsequent hidden layer. For each possible hidden layer under this two-thirds descending rule, we also created a model which maps that hidden layer directly to an output layer. For example, if a model had 9 input variables, we would make (1) a one-hidden-layer neural network with six neurons and (2) a two-hidden-layer neural network with six neurons in the first hidden layer and four hidden neurons in the second/final hidden layer. **Figure 1** displays this model-building architecture, and contains a multivariable linear regression for reference. This same approach was repeated, omitting tornado events which caused no property damage, to provide an evaluation of the predictive performance conditioned on the premise that a tornado caused damage (hereafter “conditional models”).

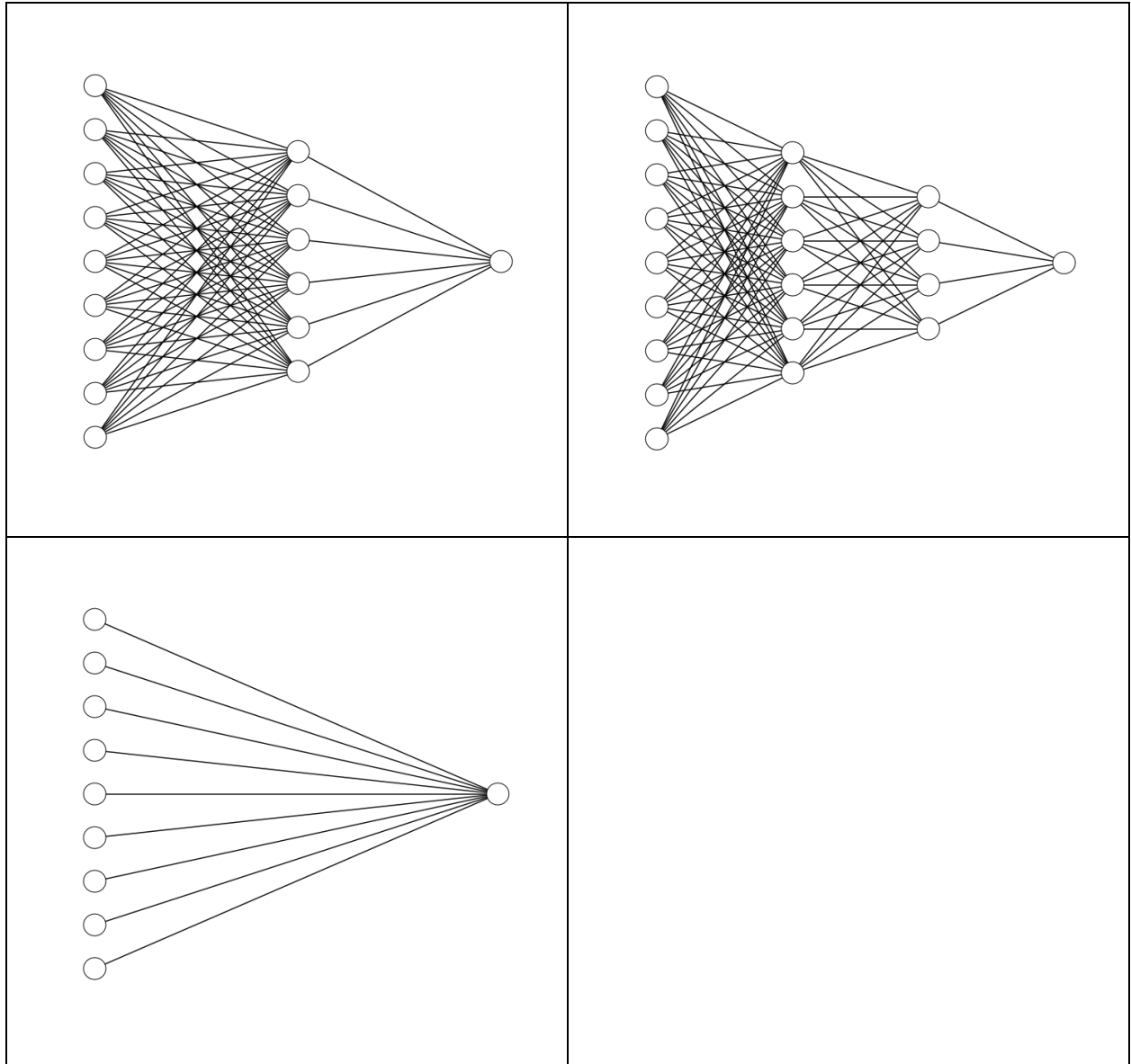


Figure 1. A representation of the descending model architecture. The top two images represent the two neural networks which would be made from 9 input variables, while the bottom image represents a linear regression for reference.

We then explored additional neural network architectures on the combined models. Rather than exclusively descending model architectures, as previously described, we tried models that were limited to 2 hidden layers but with a variable number of neurons (“wide models”) and models that were limited to 26 neurons (the ceiling-rounded result of dividing the number of input variables by two) but with variable number of hidden layers (“deep models”).

Wide models with greater than 35 neurons per hidden layer displayed overfitting, as displayed in **Figure 2b**, so we implemented dropout regularization [34], where each hidden unit may be randomly set to zero with a predefined probability during parameter optimization. The dropout probability hyperparameter was varied with the goal of choosing an optimal value.

Additionally, we evaluated the performance of models regularized by a combination of L2 and dropout regularization; the L2 regularization strength was varied logarithmically and evaluated.

These same three combined model architectures (descending, wide, and deep) were then tested on models using the exponential linear unit activation function (ELU) in place of ReLU.

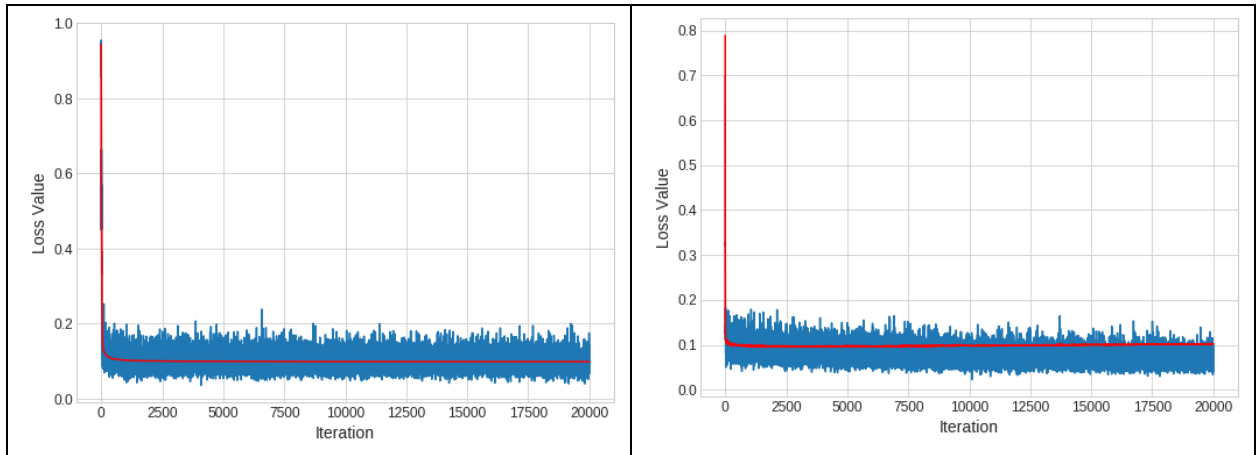


Figure 2. Comparison of model fitting when a) the models optimize well and b) when the models display overfitting. Blue line: mini-batch, training set mean squared error (MSE). Red line: cross-validation set MSE. Notice in a) that the red line stays centered within the blue line's variation, while in b) the red line is increasing relative to the blue line's center of variation.

In addition to the neural networks aimed at predicting property damage, we created a one-hidden-layer neural network to predict whether or not a tornado will cause damage (hereafter “damage classifier”). The hidden layer had 26 neurons and used a ReLU activation function, while the one-neuron output layer used a logistic activation function, providing a probability of causing damage. This probability was multiplied by the best conditional model's outputs to derive the expected value of tornado-induced property damage.

2.5. Dashboard

A grid of evenly spaced points was created for the continental United States. All geospatial and social variables were determined for these points, and mean values were assigned for storm characteristic variables; except for “Multivortex Indicator”, which was assigned 0 - indicating a non-multivortex tornado. Each point was sampled 12 times, once for the 15th of each month. This process was also done for 261 US cities that had a 2014 population exceeding 100,000. Lastly, using the best conditional model architecture and the damage classifier, we created an interactive map for the 2018 expected values for these points and cities.

All code files and notebooks to reproduce our work (data handling, analysis, and visualization) are publicly available at <https://github.com/jdiaz4302/tornadoesr/>, and, all necessary data for replication and innovation is publicly available at [35].

3. Results and Discussion

The neural network that predicted whether a tornado causes property damage was highly accurate (test set accuracy = 0.827 and test set AUROC = 0.872), and, conditional on non-zero property damage, the model that combined socioeconomic factors with physical properties of the tornado performed best (**Table 2**). By using a combination of a binary classifier, which predicts whether damage occurs for all observations, and a second-stage model that predicts the amount of damage conditional on damage having occurred (approximately 70% of the dataset), we are able to make use of the entire dataset and derive expected values for tornado induced property damages for all observations. This two step approach was preferred to models that included zero and nonzero property damages together, as it explicitly accounts for zero inflation in the property damage data.

Model performance was relatively insensitive to hyperparameter choice (**Figure 3** and **Table 2**). The best-performing model (cross-validation MSE = 0.089 and test MSE = 0.094) was a wide network using 50 neurons in each of two hidden layers, regularized with 15% dropout after each hidden layer, and its test performance is visualized in **Figure 4**.

In the combined models, overall MSE was always better than MSE for damages over 1 million USD (**Table 2**). We attempted to solve this by oversampling the extreme events during optimization, however this oversampling only changed the bias in the model via a mean-shift, where the model predicted higher damages for all tornadoes. Underestimation at the upper extremes is a notable obstacle, as the log transformation leads to numerical stability during training, but sacrifices information contained in the natural scale of the response. For example, predicting \$27 in damage when the actual value is \$10 leads to equivalent squared error loss on the log scale as predicting \$367,879 in damage when the actual value is \$1,000,000, despite the first prediction being wrong by \$17 dollars, and the second prediction being wrong by over \$600,000. Future work may benefit from combining a deep learning approach with extreme value approaches that model heavy tails without relying on log transformations, e.g., estimating the parameters of the generalized Pareto distribution with a neural network for exceedances over a threshold amount of damage [36].

Cross-Validation Set Performance

Units = log₁₀ US dollars

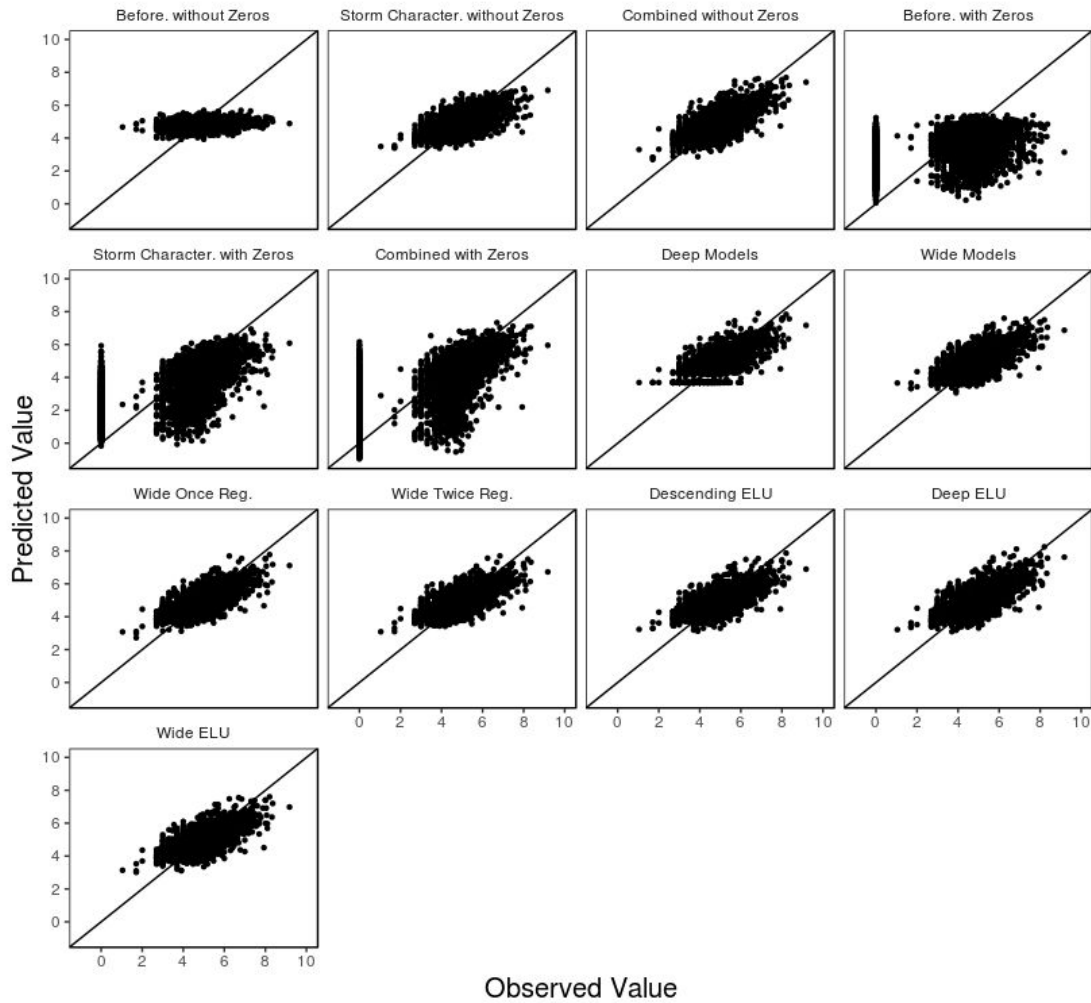


Figure 3. The best performing model of each model type. See Table 2 for performance metrics. “Before.” models utilize input variables that can be known before a tornado event, “Storm Character.” models utilize input variables that characterize the tornado, and “Combined” models combine these two sets of input variables. “... without Zeros” models do not consider the possibility of non-damaging tornadoes, “... with Zeros” models consider both non-damaging and damaging tornadoes, and all figures which do not specify “... with(out) Zeros” is a “... without Zeros” model. “Deep” models had a fixed 26 hidden units per hidden layer and explored various hidden layer depths, “Wide” models have a fixed 2 hidden layers and explored various hidden unit widths, and “Descending” models explored all possible architectures possible with a ½ descending number of hidden units in the subsequent hidden layer. “ELU” refers to the use of exponential linear unit activation functions, while non-ELU models used rectified linear unit activation (ReLU) functions.

Label	Mean Squared Error	R-squared	Mean Squared Error Over 1M	Number of Parameters
Before. with Zeros	0.7770	0.2320	1.470	599
Storm Character. with Zeros	0.6360	0.3720	0.567	749
Combined with Zeros	0.5170	0.4900	0.374	2597
Before. without Zeros	0.1610	0.0442	0.582	679
Storm Character. without Zeros	0.1060	0.3700	0.268	477
Deep Models	0.0937	0.4440	0.185	18227
Wide Models	0.0929	0.4480	0.175	1481
Combined without Zeros	0.0920	0.4540	0.171	2597
Deep ELU	0.0915	0.4570	0.155	7697
Descending ELU	0.0905	0.4620	0.182	2949
Wide ELU	0.0904	0.4640	0.179	5201
Wide Twice Reg.	0.0897	0.4670	0.191	5201
Wide Once Reg.	0.0894	0.4690	0.190	5201

Table 2. The performance metrics for the best performing models of each type, see Figure 3 for plots of predicted versus observed values. “Before.” models utilize input variables that can be known before a tornado event, “Storm Character.” models utilize input variables that characterize the tornado, and “Combined” models combine these two sets of input variables. “... without Zeros” models do not consider the possibility of non-damaging tornadoes, “... with Zeros” models consider both non-damaging and damaging tornadoes, and all figures which do not specify “... with(out) Zeros” is a “... without Zeros” model. “Deep” models had a fixed 26 hidden units per hidden layer and explored various hidden layer depths, “Wide” models have a fixed 2 hidden layers and explored various hidden unit widths, and “Descending” models explored all possible architectures possible with a % descending number of hidden units in the subsequent hidden layer. “ELU” refers to the use of exponential linear unit activation functions, while non-ELU models used rectified linear unit activation (ReLU) functions.

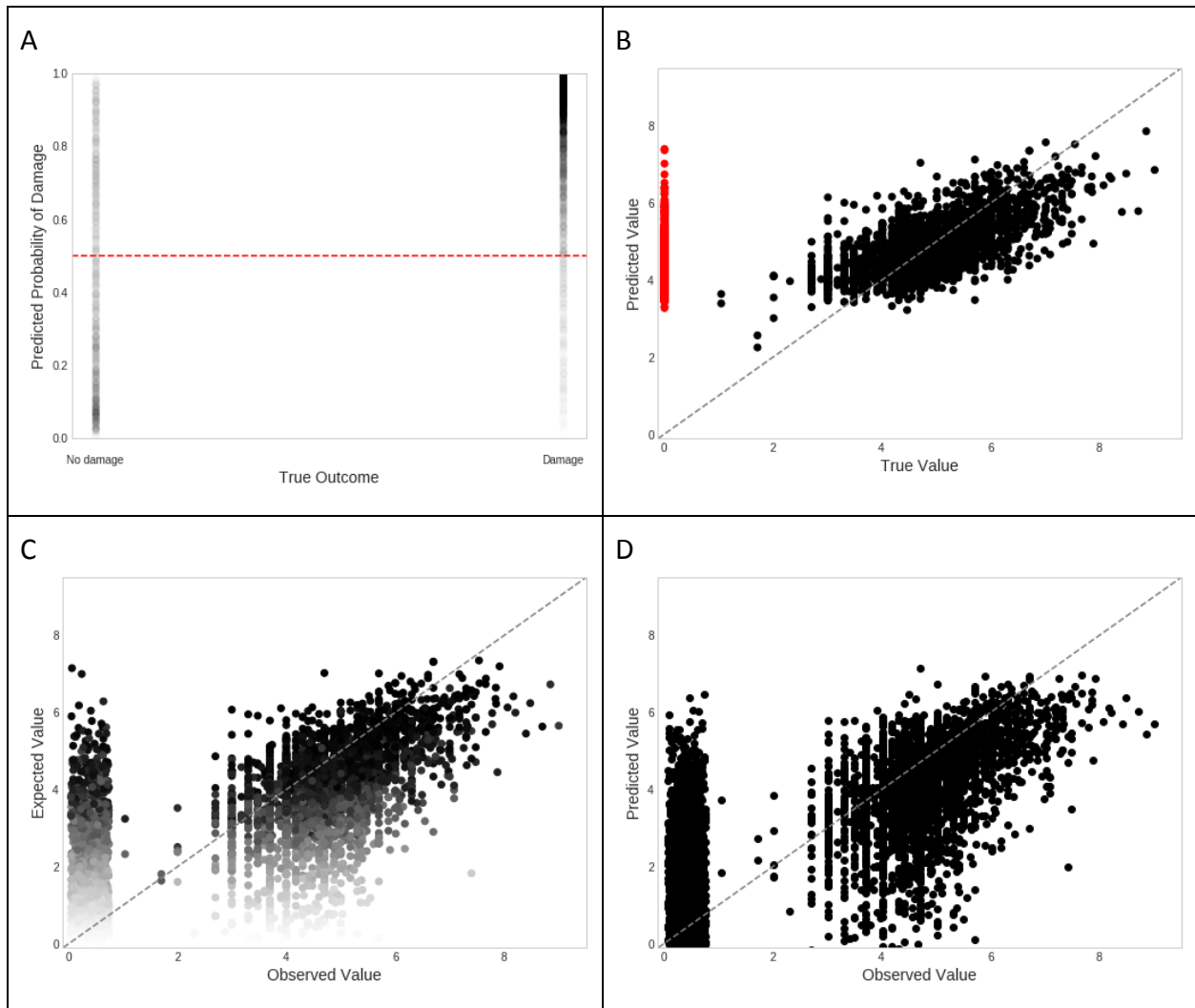


Figure 4. The best model's predictive performance on test set data. A) is the damage classifier's performance, where constant transparency is applied to more accurately represent performance. B) is the conditional model's performance, where non-damaging tornadoes are "out-of-scope" yet displayed in red. C) is the expected value model's performance, where transparency is controlled by the probability of damage (dark points indicate high probability). D) is the original model's performance, which considered non-damaging events during optimization.

The test set residuals are displayed geographically in **Supplement 1** (available at: https://rawgit.com/jdiaz4302/tornadoesr/master/interactive_model_maps.html). This map appears to display spatial regions prone to overestimating and underestimating, perhaps suggesting the absence of omitted spatially-correlated variables which have evaded our efforts and perhaps the literature. This may also be a result of the broad model scale; perhaps models with a smaller spatial extent or more rich spatial structure would perform better in these areas, as they would not perform complete pooling of the estimated effects across a large

heterogeneous region. Additionally, expected values for the 2018 year are displayed interactively in **Supplement 1** and statically in **Figure 5**.



Figure 5. Map of tornado damage expected value predictions for the 15th of each 2018 month. Produced using the best performing conditional model and the classifier. If possible, variables were derived (such as population density), otherwise (such as for "time of day") mean values were used.

There were problems which arose from working with multiple large data sets. When integrating the USCB and ACS data sets, there were a small number of county-state name inconsistencies, which led to the loss of data by the introduction of missing values; this occurred for less than 1% of events. There were also year limitations brought about by scheduled gaps from NLCD data and the fact that ACS 5-year estimates do not predate 2009 nor do they yet exist beyond 2015. For missing years, we decided to assume no change before or from adjacent years. Interpolation would provide an alternative approach, but this would considerably expand the modeling effort and require many more assumptions about how these drivers evolve in space and time.

There is a sizable literature on tornado community risk, yet this only provides us with a relative understanding of the potential community losses. Here we directly provide the continuous US dollar amount that is at risk from a tornado, providing clear socioeconomic value. In addition, we exclusively used publicly available data and software with the hope that this will promote and aid further improvements on these meaningful models, of which there are hundreds of millions of potential stakeholders.

While this paper aims at predicting *tornado*-induced property damage, the high level workflow can be repurposed to include other natural disasters. This workflow consists of two major components: 1) identify and gather risk variables, and 2) use known events to develop predictive models. Storm Events alone contains 48 different event types, and in the modern world of increasing GDP and population, these models would be of great value.

3.1. Conclusions

While there has been substantial research done in describing the characteristics of tornadoes and identifying variables of tornado risk, predicting the economic damage that they cause or threaten to American communities remains difficult. Here we show the potential that publicly available data sources and artificial neural networks have in such predictions, particularly that shallow neural networks consisting of location and non-meteorological storm characteristics provide promising performance. We also provide supplemental predictions for the year 2018 to convey the real-world value of these models.

4. Acknowledgements

This research was made possible by the University of Colorado Boulder Grand Challenge initiative and the open source software community, with special thanks to the following open source softwares: R (language - <https://www.r-project.org/>), python (language - <https://www.python.org/>), tidyverse (R packages - <https://www.tidyverse.org/>), tidycensus (R package - <https://walkerke.github.io/tidycensus/>), scipy (python packages - <https://scipy.org/>), rspatial (R packages - <http://www.rspatial.org/>), plot.ly (<https://plot.ly/>), and PyTorch (python framework - <https://pytorch.org/>).

5. References

1. Stanley A. Changnon. Natural Hazards Review. Tornado Losses in the United States. 2009. Volume 10. Pages 145-150.
2. Storm Prediction Center. The 10 Costliest U.S. Tornadoes since 1950... in event year and 2015 dollars. Available at: [http://www.spc.noaa.gov/faq/tornado/damage\\$.htm](http://www.spc.noaa.gov/faq/tornado/damage$.htm)
3. Kenneth E. Kunkel, Roger A. Pielke Jr., and Stanley A. Changnon. Bulletin of the American Meteorological Society. Temporal Fluctuations in Weather and Climate Extremes That Cause Economic and Human Health Impacts: A Review. 1999. Volume 80. Pages 1077-1098.

4. Stanley A. Changnon, Roger A. Pielke Jr., David Changnon, Richard T. Sylves, and Roger Pulwarty. Bulletin of the American Meteorological Society. Human Factors Explain the Increased Losses from Weather and Climate Extremes. 2000. Volume 81. Pages 437-442.
5. American Meteorological Society. Mobile Homes and Severe Windstorms. Available at: <https://www.ametsoc.org/ams/index.cfm/about-ams/ams-statements/archive-statements-of-the-ams/mobile-homes-and-severe-windstorms/>
6. Olivia Kellner and Dev Niyogi. Earth Interactions. Land Surface Heterogeneity Signature in Tornado Climatology? An Illustrative Analysis over Indiana, 1950–2012. 2014. Volume 18. Paper number 10. Pages 1-32.
7. Walker S. Ashley and Stephen M. Strader. Bulletin of the American Meteorological Society. RECIPE FOR DISASTER: How the Dynamic Ingredients of Risk and Exposure Are Changing the Tornado Disaster Landscape. 2016. Volume 97. Pages 767-786.
8. Walker S. Ashley, Stephen Strader, Troy Rosencrants, and Andrew J. Krmenc. Weather, Climate, and Society. Spatiotemporal Changes in Tornado Hazard Exposure: The Case of the Expanding Bull's-Eye Effect in Chicago, Illinois. 2014. Volume 6. Pages 175-193.
9. David R. Godschalk. Natural Hazards Review. Urban Hazard Mitigation: Creating Resilient Cities. 2003. Volume 4. Pages 136-143.
10. Javier Salmerón and Aruna Apte. Production and Operations Management. Stochastic Optimization for Natural Disaster Asset Prepositioning. 2010. Volume 19. Pages 561-574.
11. David J. Stensrud, Ming Xue, Louis J. Wicker, Kevin E. Kelleher, Michael P. Foster, Joseph T. Schaefer, Russell S. Schneider, Stanley G. Benjamin, Stephen S. Weygandt, John T. Ferree, and Jason P. Tuell. Bulletin of the American Meteorological Society. Convective-scale Warn-on-forest system: A vision for 2020. 2009. Volume 90. Pages 1487-1499.
12. David A. McEntire. Disaster Prevention and Management: An International Journal. Coordinating multi-organisational responses to disaster: lessons from the March 28, 2000, Fort Worth tornado. 2002. Volume 11. Pages 369-379.
13. Kahn, Matthew E. "The death toll from natural disasters: the role of income, geography, and institutions." The Review of Economics and Statistics 87.2 (2005): 271-284. Available at: <https://www.mitpressjournals.org/doi/abs/10.1162/0034653053970339>
14. Kurt Hornik. Neural Networks. Approximation Capabilities of Multilayer Feedforward Networks. 1991. Volume 4. Pages 251-257.
15. Kurt Hornik. Neural Networks. Multilayer Feedforward Networks are Universal Approximators. 1989. Volume 2. Pages 359-366.
16. Caren Marzban and Gregory J. Stumpf. Journal of Applied Meteorology and Climatology. A Neural Network for Tornado Prediction Based on Doppler Radar-Derived Attributes. 1996. Volume 35. Pages 617-626.
17. Caren Marzban. Neural Computing and Applications. A Neural Network for Tornado Diagnosis: Managing Local Minima. 2000. Volume 9. Pages 133-141.

18. Caren Marzban and Gregory J. Stumpf. Weather and Forecasting. A Neural Network for Damaging Wind Prediction. 1998. Volume 13. Pages 151-163.
19. Matthew J. Aitkenhead, Parivash Lumsdon and David R. Miller. Disasters. Remote sensing-based neural network mapping of tsunami damage in Aceh, Indonesia. 2007. Volume 31. Pages 217-226
20. Andre Zergera and David Ingle Smith. Computers, Environment and Urban Systems. Impediments to using GIS for real-time disaster decision support. 2003. Volume 27. Pages 123-141
21. National Centers for Environmental Information. Storm Events Database. 1997-2017. Dataset identifiers: NCEI DSI 3910_03, gov.noaa.ncdc:C00510.
22. Daniel McCarthy. 1st Symposium on the F-Scale and Severe-Weather Damage Assessment. NWS Tornado Surveys and the Impact on the National Tornado Database. 2003. Section 3.2. Pages 1-7.
23. Homer, C., Dewitz, J., Fry, J., Coan, M., Hossain, N., Larson, C., Herold, N., McKerrow, A., VanDriel, J.N., and Wickham, J. 2007. Completion of the 2001 National Land Cover Database for the Conterminous United States. *Photogrammetric Engineering and Remote Sensing*, Vol. 73, No. 4, pp 337-341.
24. Fry, J., Xian, G., Jin, S., Dewitz, J., Homer, C., Yang, L., Barnes, C., Herold, N., and Wickham, J., 2011. Completion of the 2006 National Land Cover Database for the Conterminous United States, *PE&RS*, Vol. 77(9):858-864.
25. Homer, C.G., Dewitz, J.A., Yang, L., Jin, S., Danielson, P., Xian, G., Coulston, J., Herold, N.D., Wickham, J.D., and Megown, K., 2015, Completion of the 2011 National Land Cover Database for the conterminous United States-Representing a decade of land cover change information. *Photogrammetric Engineering and Remote Sensing*, v. 81, no. 5, p. 345-354
26. U.S. Census Bureau; American Community Survey, 2009-2015 American Community Survey 5-Year Estimates, Tables B25024_010E, B01003_001E, and B19013_001E; generated by Jeremy Diaz using the American Community Survey API via the R package tidycensus.
27. U.S. Census Bureau; USA Counties Data File Downloads - Land Area, Table LND010200D. Available at: <https://www.census.gov/support/USACdataDownloads.html>.
28. Storm Prediction Center. Multiple Vortex Tornado. Available at: <http://www.spc.noaa.gov/faq/tornado/altus.htm>
29. Walker S. Ashley. Weather and Forecasting. Spatial and Temporal Analysis of Tornado Fatalities in the United States: 1880–2005. 2007. Volume 22. Pages 1214-1228.
30. Peggy R. Concannon, Harold E. Brooks, and Charles A. Doswell III. Second Conference on Environmental Applications, American Meteorological Society. CLIMATOLOGICAL RISK OF STRONG AND VIOLENT TORNADOES IN THE UNITED STATES. 2000. Paper 9.4. Available at: http://www.nssl.noaa.gov/users/brooks/public_html/concannon/

31. Harold E. Brooks, Charles A. Doswell III, and Michael P. Kay. Weather and Forecasting. Climatological Estimates of Local Daily Tornado Probability for the United States. 2003. Volume 18. Pages 626-640.
32. The National Severe Storms Laboratory. Severe Weather 101: Tornadoes. Available at: <http://www.nssl.noaa.gov/education/svrwx101/tornadoes/>
33. John Duchi, Elad Hazan, and Yoram Singer. Journal of Machine Learning Research. Adaptive Subgradient Methods for Online Learning and Stochastic Optimization. 2011. Volume 12. Pages 2121-2159.
34. Nitish Srivastava, Geoffrey Hinton, Alex Krizhevsky, Ilya Sutskever, and Ruslan Salakhutdinov. Journal of Machine Learning Research. Dropout: A Simple Way to Prevent Neural Networks from Overfitting. 2014. Volume 15. Pages 1929-1958. Available at: <http://jmlr.org/papers/v15/srivastava14a.html>
35. Diaz, Jeremy (2018): Data for "Predicting property damage from tornadoes with deep learning". figshare. Dataset. Available at: <https://doi.org/10.6084/m9.figshare.6792206.v4>
36. Julie Carreau and Yoshua Bengio. *IEEE Transactions on Neural Networks*. A Hybrid Pareto Mixture for Conditional Asymmetric Fat-Tailed Distributions. 2009. Volume 20. Pages 1087-1101